

目 录

中文摘要	I
英文摘要	VI
第一章 绪论	1
§ 1-1 拉曼光谱.....	1
§ 1-1-1 拉曼光谱的发现	1
§ 1-1-2 拉曼光谱效应	1
§ 1-1-3 拉曼光谱的发展.....	3
§ 1-2 表面增强拉曼光谱的发现及特点.....	4
§ 1-3 表面增强拉曼光谱的局限性及其发展.....	6
§ 1-4 表面增强拉曼光谱在纯过渡金属体系的拓宽及应用.....	7
§ 1-4-1 SERS 金属基底的制备方法.....	7
§ 1-4-2 过渡金属体系表面的 SERS 研究.....	9
§ 1-5 表面增强拉曼效应机理.....	12
§ 1-5-1 电磁场增强效应.....	13
§ 1-5-2 化学增强效应.....	21
§ 1-6 实验目的和设想.....	27
参考文献	29
第二章 实验研究方法.....	33
§ 2-1 共焦显微拉曼谱仪.....	33
§ 2-2 原子力显微镜(AFM).....	36
§ 2-3 扫描电子显微镜(SEM).....	38

§ 2-4 实验试剂、气体和仪器	40
参考文献	41
第三章 金属钴的表面增强拉曼散射效应	42
§3-1 实验方法.....	43
§3-2 金属钴的表面粗糙.....	44
§3-3 钴粗糙电极表面增强因子的估算.....	47
§3-3-1 钴粗糙电极表面粗糙度的估算.....	47
§3-3-2 利用共焦显微拉曼系统估算粗糙钴电极表面的 SERS 增强因子	48
§3-4 金属钴的表面拉曼增强机理.....	52
§3-4-1 电磁场增强机理.....	52
§3-4-2 电荷转移机理.....	56
本章小结	60
参考文献.....	61
第四章 苯骈三氮唑 (BTA) 对钴的缓蚀机理的电化学 SERS 和量子 化学研究.....	127
§4-1 金属钴的应用以及腐蚀性能.....	63
§4-2 金属钴的腐蚀及缓蚀的研究现状.....	64
§4-3 不同 pH 值的 BTA 拉曼溶液谱的指认.....	67
§4-3-1 实验.....	68
§4-3-2 计算方法.....	69
§4-3-3 BTA 三种存在形式的溶液 Raman 谱和 BTAH 固体 Raman 谱	71

§4-3-4 BTAH/D 固体 Raman 谱的振动模式的指认·····	72
§4-3-5 三种 BTA 存在形式分子的溶液 Raman 谱的指认·····	75
§4-4 BTA 在不同 pH 值溶液中对钴的缓蚀作用机理·····	80
§4-4-1 实验·····	80
§4-4-2 酸性溶液中 BTA 对钴的缓蚀作用机理·····	82
§4-4-3 中性溶液中 BTA 对钴的缓蚀作用机理·····	89
§4-4-4 碱性溶液中 BTA 对钴的缓蚀作用机理·····	95
本章小结 ·····	100
参考文献 ·····	101
第五章 金属钴纳米线阵列的 SERS 研究·····	105
§ 5-1 多孔氧化铝模板的形成机理·····	107
§ 5-1-1 多孔氧化铝模板的结构和生长机理·····	108
§ 5-1-2 影响多孔氧化铝模板结构的条件·····	109
§ 5-2 多孔氧化铝模板的制备·····	111
§ 5-3 交流电沉积法制备金属 Co 纳米阵列·····	113
§ 5-4 Co 纳米阵列的 SERS 研究·····	118
§ 5-4-1 Co 纳米阵列的获得·····	118
§ 5-4-2 Co 纳米阵列的 SERS 行为·····	127
§ 5-4-3 Co 纳米阵列的 SERS 机理研究·····	130
§ 5-4-4 对实验的一些想法·····	136
本章小结 ·····	138
参考文献 ·····	140
作者攻读硕士学位期间发表与交流论文 ·····	142
致谢 ·····	144

金属钴的表面增强拉曼光谱应用 及其增强机理的初步探索

中文摘要

拉曼 (Raman) 光谱作为一种分子振动光谱, 受溶剂水的影响很小, 很适合从分子水平上对固 - 液、气 - 液等表面, 特别是电化学界面进行现场研究。但大多数表面单层吸附物种的拉曼信号强度都低于常规谱仪的检测灵敏度, 很大程度上限制了拉曼光谱在电化学研究中的应用。表面增强拉曼散射 (Surface-enhanced Raman scattering, 简称 SERS) 效应的发现, 使得吸附物种在特定的电极表面存在约 10^6 的表面增强, 极大的提高了检测灵敏度。但是二十多年过去了, 表面增强拉曼光谱技术并未如最初所期望那样发展成为重要且得到广泛应用的表面科学工具, 究其原因, 主要由于它存在以下三方面的问题而严重制约了它的发展:

(i) 人们通过系统和全面的研究, 遗憾地发现仅有三种币族金属 (Ag、Au 和 Cu) 以及少数极不常用的碱金属 (如锂、钠等) 才具有强的表面增强效应, 这严重地限制了表面增强拉曼光谱的应用体系。

(ii) SERS 技术的前提是必须对电极进行适当的粗糙化以获得具有 SERS 活性的表面。虽然具有 SERS 活性的粗糙表面与实际应用体系较为接近, 但其表面结构十分复杂。这给制备可重现的粗糙表面以及应用 SERS 开展定性 (例如吸附取向、表面选律等) 和定量研究带来极大的困难。

(iii) SERS 机理迄今仍未完全被揭示。粗糙表面同时具有宏观 (几十到几百纳米) 和微观 (原子或原子簇) 的表面粗糙度, 这两种表面粗糙度分别对应着物理增强和化学增强这两大主要机理, 复杂的粗糙表面使得人们在实验上得到的往往是这两种增强效应对 SERS 的综合贡献。此外, 在理论上难以对粗糙表面的真实几何构型和能级结构进行直接描述, 无法全面的描述入射光、金属基底和表面物种复杂的相互作用, 因此难于从理论上对这两

种增强方式的贡献下定论。

针对 SERS 应用中遇到的上述三大障碍, 本论文从金属钴(Co)体系入手, 将实验和理论相结合, 研究了具有三个数量级增强效应的粗糙 Co 电极表面的 SERS 机理, 并以缓蚀剂苯并三氮唑 (Benzotriazole, BTA) 作为探针分子, 探索将 SERS 技术应用到 Co 的表面缓蚀、电化学腐蚀行为的研究; 为了克服粗糙表面形貌无序的缺点, 利用电化学模板沉积技术制备了尺度可控的 Co 纳米线阵列, 探索将这种阵列作为高活性的 SERS 基底以及研究 SERS 机理模型的可能性。本论文的主要研究结果可归纳如下:

一、纯钴金属粗糙表面的 SERS 机理研究

在我们小组使用的粗糙过渡金属电极方法的基础上, 采用电化学氧化还原 (ORC) 方法, 并结合化学刻蚀, 获得具有较强 SERS 活性和重现性较好的 Co 电极表面, 其表面积约为光亮电极的 2.7 倍。由 AFM 表征得知, 粗糙 Co 电极表面是由许多 300~400 nm 的粒子堆积而成, 而这些粒子又是由小于 50 nm 的颗粒组成。在此表面上获得了吸附吡啶分子的高质量拉曼谱, 排除因表面积增大导致的表面信号增强的因素后, 计算出该体系的增强因子(G)约为三个数量级。

结合实验数据, 分别从表面电磁场增强机理(EM)和电荷转移增强机理(CT)两个角度对增强因子进行了的估算。利用长短轴之比为 2 的二维纳米椭圆阵列模型, 计算出在 400~2000 nm 的激发波长范围内阵列表面局域电场对表面增强因子的贡献为 3 个数量级, 但表面共振增强的特性并不明显。考虑到计算模型的局限性, 估计 EM 机理对 Co 电极表面 SERS 增强因子的贡献大约为 1~2 个数量级。

为了验证是否存在电荷转移增强机理, 我们利用 632.8 nm 及 514.5 nm 激光检测了吸附吡啶的 SERS 随电极电位的变化, 发现随着激发光频率的蓝移, 吡啶信号强度峰值电位的发生正移。这说明吸附在 Co 电极上的吡啶的 SERS 信号包含着电荷转移增强的贡献, 并且电荷是从金属向吸附分子转移。理论分析表明, 电荷转移过程中电子存在着两种跃迁过程: 电子从金属的 Fermi 能级激发到 Py 分子未占据 π 轨道的 $B_1(\pi^*)$ 和 $A_2(\pi^*)$ 上,

其中 $A_2(\pi^*)$ 的轨道能量大约比 $B_1(\pi^*)$ 高 0.3 eV, 这与实验中观察到的两个峰值电位的相对位置一致。通过计算可以得出电荷转移增强对 SERS 的贡献为一个数量级。以上结果表明, Co 电极表面吡啶吸附的 SERS 效应包含以上两种增强机理的贡献。

二、苯骞三氮唑对金属钴缓蚀作用的电化学 SERS 和量子化学研究

采用具有 SERS 活性的粗糙 Co 电极表面作为基底, 将 SERS 技术和传统电化学方法相结合, 现场研究了不同 pH 值溶液中 BTA 对金属 Co 的缓蚀以及电化学腐蚀行为。

BTA 有三种存在形式, 分别为 $BTAH_2^+$ 、 $BTAH$ 和 BTA^- 。由于 BTA 具体的存在形式取决于溶液的 pH 值、溶液的组分、电极电位、电极材料等因素, 故而 BTA 对金属的缓蚀作用机理因腐蚀环境的不同而显得十分复杂。因此为了更好的利用 SERS 光谱技术来研究 BTA 对 Co 缓蚀行为, 必须对 BTA 不同存在形式的溶液谱中各振动模式有较好的归属。在得到高质量的溶液谱和 BTAH 固体谱的实验基础上, 结合 Gaussian 98 *ab initio* Hartree-Fock (HF) 方法 (6-31G**基组) 对上述三种分子的振动分析, 对 BTA 三种存在形式溶液谱中各振动模式进行了较为完整的指认。

通过电化学稳态技术测量粗糙 Co 电极在含有 BTA 的酸、中、碱性溶液中的 Tafel 曲线, 发现 BTA 在酸、中、碱性溶液中对金属 Co 都具有缓蚀作用, 且随着浸泡时间的延长其缓蚀效率不断的提高。在中性溶液中 BTA 的缓蚀效率最高, 酸性溶液其次, 碱性溶液最低。采用 SERS 技术现场跟踪开路电位下不同 pH 值环境中 BTA 对金属 Co 的缓蚀过程, 发现 BTA 是一种成膜型缓蚀剂, 随着浸泡时间的延长缓蚀层的厚度不断增加。在酸性溶液中, 缓蚀层是由 $BTAH_2^+$ 、 $BTAH$ 通过三氮环上 N 原子的孤对电子和 Co 空的 d 轨道形成配位键构成的; 在中性溶液中, BTA 是以碱性分子 BTA^- 与金属 Co 的氧化物 Co^{III} 形成配合物缓蚀层 $[Co(BTA)_x]_p$, 同样是通过三氮环上 N 原子的孤对电子和 Co 空的 d 轨道形成配位键; 在碱性溶液中, BTA^- 通过与 OH 和溶解氧的协同作用对金属 Co 产生缓蚀作用, 使金属 Co 氧化在表面上形成以 CoO 为主要成分的氧化物钝化层阻碍 Co 的进一步氧化。

对金属 Co 在不同 pH 值溶液中形成了缓蚀层后的电化学腐蚀行为进行了现场 SERS 研

究。在酸性溶液中，Co 的氧化腐蚀过程是一个渐变的过程：在未达到腐蚀电位的情况下，随着电极电位的正移，Co-N 的配位键逐渐被削弱，缓蚀层的厚度不断减小，其中的 BTAH_2^+ 由于静电作用不断转变成 BTAH。当达到腐蚀电位时，缓蚀层基本上被分解完全，Co 氧化生成 Co^{2+} 与 SO_4^{2-} 化合生成微溶性的 CoSO_4 ，聚集在 Co 电极表面。在中性溶液中，Co 表面并没有形成氧化物，其氧化的产物 Co^{n+} 与 BTA 形成配合物，并随着电极电位的不断正移，在电极表面上发生交替的聚集和溶解。在碱性溶液中，Co 的电化学氧化过程是一个突变的过程，只有当电极电位正移至腐蚀电位时，缓蚀层才被破坏分解。

三、金属钴纳米线阵列的 SERS 研究

粗糙 SERS 活性表面存在着粒子大小形状不一、排列无序杂乱等问题，不利于 SERS 的定性和定量分析，并难以区分电磁场增强和化学增强两种效应对 SERS 的贡献。因此我们以在草酸溶液中直流氧化的多孔氧化铝为模板，采用交流电沉积的方法，制备了直径与模板孔洞尺度一致、填充率为 60~70%、从模板阻挡层开始生长的 Co 纳米线阵列。采用 H_3PO_4 和 NaOH 交替溶解的方法，从模板的阻挡层开始溶解，可以得到长径比为 1:1~1:5 的 Co 纳米棒阵列。采用 SCN^- 为表面探针分子，以波长为 632.8 nm 的激光为激发光，表征了不同长径比的 Co 纳米阵列表面的 SERS 行为，发现随着长径比的增加增强因子出现先增后减的变化趋势，长径比为 2:1 的具有最大的 SERS 效应，计算结果表明存在约 1 个数量级的表面增强效应。该现象无法以探针分子的吸附取向和表面覆盖度的变化、电荷转移增强效应以及有效表面积增加来解释，因为 SCN^- 足以在表面形成满单层吸附并且实验中入射光子的能量保持不变。根据二维纳米椭球阵列的模拟计算，得出金属阵列的表面等离子体增强效应随着阵列长径比的增加（1:1~1:4）不断增加。针对引起实验和理论结果的偏差的原因进行了讨论，认为该实验现象可能归属于表面等离子体增强效应和阵列表面存在着氧化物的综合贡献，但无法判断避雷针效应是否对该实验现象有贡献。

由于 Co 纳米阵列表面难以避免生成表面氧化物，导致理论计算难以解释得到的实验现象。为了克服这一困难，可采用以下两种方法制备具有导电层可控制电位的 Co 纳米阵

列：一种方法是采用直流电沉积的方法，另一种方法就是在交流电沉积的基础上在进行化学镀。采用这种表面形貌有序、尺度可控、可以施加电极电位的金属纳米阵列为 SERS 基底，结合更有效准确的理论模型进行理论计算，有望进一步推动 SERS 增强机理的研究。

本论文以将 SERS 应用到过渡金属 Co 体系为中心，首先对具有三个数量级 SERS 活性的粗糙 Co 电极表面进行了 SERS 机理研究，理论分析认为粗糙表面的 SERS 效应来自于电磁场增强和电荷转移增强两者的贡献。然后以该粗糙电极表面为 SERS 研究的基底，将 SERS 和传统电化学技术相结合，研究了缓蚀剂分子 BTA 在 Co 表面成膜和电化学腐蚀过程，初步解释了 BTA 对 Co 的缓蚀机理，认为 BTA 通过在 Co 电极表面形成缓蚀层而达到缓蚀的效果，实质性的将 SERS 技术应用到过渡金属 Co 体系中。为了克服粗糙表面给 SERS 技术带来的分析和机理研究上的问题，制备了表面形貌有序、尺度可控的 Co 纳米阵列，在该阵列表面得到了 1 个数量级的表面增强效应。由于硕士工作期间时间有限，还无法对 Co 纳米阵列的 SERS 行为及其机理进行详细的研究。针对本论文工作存在的问题，提出了一些实验设想，以期进一步促进 SERS 增强机理理论研究的进程。

Application of Surface-enhanced Raman Spectroscopy on Cobalt and a Preliminary Investigation in the Surface Enhancement Mechanism

ABSTRACT

As a molecular vibrational spectroscopy, Raman spectroscopy is very suitable for the investigation of solid/liquid and gas/liquid interfaces, especially electrochemical interfaces, due to the negligible interference of water signal to the desired Raman signal. However, Raman intensities of most adsorbates are below the detection sensitivity of conventional Raman spectrometers, which greatly limits its application on electrochemistry. The discovery of surface-enhanced Raman scattering (SERS) effect, which can enhance the Raman scattering process of an adsorbate on a certain metal surface by a factor of six orders of magnitude, significantly improves the detection sensitivity of Raman spectroscopy. However, even about 25 years after the discovery of SERS, it has not yet been developed into a general and important tool for surface sciences as expected in its infant stage. The following three problems of SERS severely limit its development :

- i) Only coinage metals (e.g., Ag, Au and Cu) and some practically seldom used alkali metals such as Li and Na exhibit great enhancement of Raman effect, which has limited severely the wide application of SERS.
- ii) The prerequisite for obtaining strong SERS is to roughen the metal electrode to obtain a SERS active surface. Roughened surfaces are close to practical systems, however, their surface structures are really complex. This results in the difficulty in preparing reproducible electrode surfaces and performing qualitative (adsorption orientation and surface selection rule) and quantitative Raman study.
- iii) The mechanism of SERS is still not clear. A SERS active surface is composed of particles with sizes ranging from several hundreds nanometer to several atoms, which contribute to the electromagnetic (EM) enhancement and charge transfer (CT) enhancement. Therefore, SERS signals obtained are normally a combined contribution of both mechanisms. Up to date, it is still difficult to simulate the geometric and energetic structure of a real roughened surface, as well as the interaction among

the incident photons, metal substrates and adsorbates. As a result, it is still ambiguous to identify the relative contribution of the two mechanisms.

To tackle the above-mentioned three problems of SERS, we devised a procedure to obtain SERS-active Co electrodes and performed corresponding SERS study. With the help of theoretical calculation, the SERS mechanism of rough Co surfaces was investigated. Using benzotriazole (BTA) as the probe molecule, SERS was applied to investigate the corrosion and inhibition process of Co electrode. In order to minimize the problem met in the system of a disorder rough surface, ordered Co nanorod arrays with controllable sizes were fabricated and used as an ideal substrate for investigation of the SERS mechanism. The main results and conclusions of this thesis are listed as follows:

(i) Investigation of the SERS mechanism of roughened Co surfaces

On the basis of the previous roughening methods for transition metals, we obtained roughened cobalt surfaces using chemical etching followed by electrochemical oxidation reduce circle (ORC). The surface presents reasonably high SERS activity and relatively good SERS reversibility, and the surface area of which is about 2.7 folds larger than that of the smooth surface. The atomic force microscopic study reveals that the rough Co surfaces consist of particles with diameters of 300~400 nm and the later are further composed of smaller particles with diameters of smaller than 50 nm. We succeeded in obtaining high-quality surface Raman spectroscopy of pyridine adsorbed on this roughened surface. The surface enhancement factor (SEF) is about 3 orders of magnitude after excluding the enhancement due to the increase of the surface area.

A theoretical calculation of the relative contribution of EM and CT has been made according to our experimental data. With the use of the model of two-dimension ellipsoidal nanoarrays with an aspect ratio of 2:1, SEF of 3 orders of magnitude from EM was calculated with laser excitation wavelength between 400 and 2000 nm. After considering the limitation of this model, SEF from EM was estimated to be 1~2 orders of magnitude.

In order to verify the contribution of CT, the potential dependent behavior of SERS of Py adsorbed on the Co surface has been investigated with 632.8 and 514.5 nm lasers. It was found that a blue shift of incident laser leads to the positive shift of the potential at maximum SERS intensity, which was an evidence of the contribution of CT to the SERS. The calculation further revealed that the charge transfers from metal to pyridine and there exist two charge transfer processes: from the Fermi level of metal to the unoccupied π orbitals, $B_1(\pi^*)$ and $A_2(\pi^*)$ of pyridine, respectively. The orbital energy of $A_2(\pi^*)$ is about 0.3 eV higher than that of $B_1(\pi^*)$. The energy difference is in agreement with the potential separation of the peak potential. The enhancement due to CT is about 1 order of magnitude. Therefore, the SERS of a rough Co surface comes

from the contribution of both EM and CT mechanisms.

(ii) Electrochemical SERS and quantum chemical study of the inhibition of benzotriazole (BTA) on the corrosion of Co electrode surfaces

Using the SERS-active roughened Co surface as the substrates and combining SERS and conventional electrochemical methods as well as quantum chemical calculation, the inhibition and electrochemical corrosion process of Co in solution of different pHs with the presence of BTA was investigated.

There are three existing forms of BTA in solutions of different pHs, the protonated cation (BTAH_2^+), neutral molecule (BTAH) and dissociated anion (BTA^-). Since the existing form of BTA depends on the solution pH, the solution composition, the electrode potential and the electrode material, the investigation of the inhibition mechanism of BTA becomes a very tough task due to the difference in the corrosion environment. In order to make full use of SERS in the investigation of the inhibition process of BTA to Co, one should have a clear assignment of the vibrational bands for different BTA existing forms. On the basis of the high quality normal Raman spectra of the BTA aqueous solution and solid, we performed vibrational analysis of the three existing forms using *ab initio* Hartree-Fock method with 6-31G** basis set. A relatively clear assignment of the vibrational modes of the three forms has been made.

With the use of electrochemical Tafel technique, it's been found that BTA behaviors as an inhibitor for Cobalt in the acidic, neutral and basic solutions, and the inhibition effect improves with the increase of the immersion time of Co electrode in BTA solutions. The inhibition effect in neutral solution is the best, followed by the acidic solution and basic solution. In-situ SERS researches of the inhibition process of BTA to Co in BTA solutions with different pHs at the open circuit potential revealed that BTA acts as an inhibitor through forming inhibition layers covering Co electrode surfaces. The thickness of the layer increases with the increase of immersion time. In the acidic solution, the inhibition layer consists of BTAH_2^+ and BTAH, and the lone electron pair of N atoms of which interacts with the unoccupied d orbit of Co atom. In the neutral solution, BTA exists as the form of BTA^- and the lone electron pair of N atom interacts with the unoccupied d orbit of Co^{n+} to form surface complex $[\text{Co}(\text{BTA})_x]_p^-$. In the basic solution, BTA^- , OH^- and the dissolved oxygen cooperatively form a Co oxides layer to protect the surface from corrosion.

The electrochemical corrosion of Co electrodes covered with inhibition layers in solutions with different pHs has been investigated with in-situ electrochemical SERS technique. In the acidic solution, the corrosion of Co is a gradual process. Before the onset of the corrosion of Co, Co-N bond is weakened with the positive shift of the electrode potential. Meanwhile the inhibition layer becomes thinner and BTAH_2^+ in the

layer transforms to BTAH due to the electrostatic effect. At corrosion potentials, the inhibition layer decomposes almost completely and surface Co atoms are oxidized to Co^{2+} . The latter combines with the surrounding SO_4^{2-} to form insoluble CoSO_4 covering the Co surface. In the neutral solution, Co is oxidized to Co^{III} , and forms surface complex $[\text{Co}(\text{BTA})_x]_p$ with BTA. With the positive shift of the electrode potential, the complex experiences an alternative decomposition and formation process. In the basic solution, the electrochemical corrosion is an instant process. Only after the occurrence of the electrochemical corrosion, the inhibition layer decomposes.

(iii) SERS study of Co nanorod arrays

Normal SERS active surfaces consist of particles with different size and shape distribution and arranged in disorder, which prevents from qualitative and quantitative analysis using SERS and separating the relative contribution of EM and CT mechanisms to SERS using theoretical model. With the use of porous alumina template prepared using direct-current oxidation method in oxalic acid, Co nanowire arrays have been obtained using alternating-current deposition method. Co nanowire arrays have the same diameter as the template with a filling ratio of 60~70%. They grow from the barrier layer of porous alumina. Co nanorod arrays with aspect ratios from 1:1 to 1:5 have been prepared by removing the porous alumina beginning from the barrier layer with the alternative dissolution using H_3PO_4 and NaOH . SERS of SCN^- adsorbed on the Co nanorod arrays with different aspect ratios has been obtained with the excitation wavelength of 632.8 nm. One order of magnitude enhancement has been found. The maximum enhancement was observed on the nanorods with the aspect ratio of 1:2. This tendency can not be explained by the orientation change of the probe molecule and the variation of the surface coverage or by the charge transfer effect and the increment of the effective surface area, because SCN^- is expected to adsorb on the surface as a monolayer under our experimental condition and the incident laser wavelength did not change.

The simulation by the two-dimension nano-ellipsoidal array reveals an increase in the EM enhanced factor of the nanorods with the increase of the aspect ratios from 1:1 to 1:4. The difference between experimental and theoretical results may be due to the enhancement effect as a result of the surface plasma resonance and existence of Co oxides on the nanorod surfaces. However, on the basis of present data, whether the contribution of lightning rod effect is still ambiguous.

Co nanorod surfaces tend to form Co oxides under ambient and aqueous solution. The existence of oxide may lead to the difference between experimental data and theoretical simulation. In order to solve this problem, one may try the following two methods to obtain a nanorod array capable of being potential controlled at cathodic

potentials: One way is to use the direct-current electrodeposition, and the other is to employ alternative-current electrodeposition followed by chemical deposition. With the use of such surface consisting of size and shape controlled particles and capable of being potential controlled, we may be able to correlate the experimental data with theoretical prediction more efficiently and accurately. This will be of help for a deeper understanding of the SERS mechanism.

In this thesis, we extend the application of SERS to Co electrode surfaces by finding a proper roughening method for Co. In order to understand the SERS mechanism on this surface, we perform theoretical calculation of the EM and CT mechanism. Both the experimental and theoretical results indicate that these two mechanisms contribute to the SERS of Co. Using the roughened Co surface with high SERS activity, we investigated the inhibition process of BTA on the corrosion of Co electrode surface and proposed the inhibition mechanism that BTA forms inhibition layer on the Co surface. In order to overcome the inherent problem of a rough surface, we fabricated ordered Co nanorod arrays with controllable size and shape, and obtained one order of magnitude of surface enhancement. Due to the time limitation during the period for M. S. studies, it is still impossible to have a very detailed investigation of the SERS behavior and mechanism. Taking account of the problems existing in present thesis, we proposed some future works in hope of a better understanding of the SERS mechanism.

第一章 绪论

§ 1.1 拉曼光谱

§1.1.1 拉曼光谱的发现

光散射是自然界的一种常见现象。当一束光照射到介质时，大部分的光被介质反射或透过介质，另一部分的光被介质向各个方向散射。光的散射包含了多种形式，最早发现的是散射频率与入射光的频率相同的瑞利 (Rayleigh) 散射和由不均匀的介质或悬浮尘埃颗粒的介质所引起的丁铎尔(Tyndall)散射。到了 1922 年人们发现介质对入射光的散射还产生一种频率发生变化的散射光，称为布里渊(Brillouin)散射，它是由于介质中存在弹性波所引起，但其频率往往变化很小，一般在 $0.1 \sim 0.2 \text{ cm}^{-1}$ ，同时人们也在理论上预测到了物质对光的非弹性散射[1-3]。直到 1928 年，印度物理学家拉曼(C. V. Raman) 利用汞灯作为光源，研究纯苯液体的光散射时通过棱镜分光后发现，在散射光中除了有与入射光频率相同的瑞利谱线外，还有与入射光频率发生位移(频率增加或减小)且强度极弱的谱线[4]，即拉曼散射光，该效应称为拉曼效应，随后也得到了其他科学家进一步的定量验证[5-8]。

§1.1.2 拉曼光谱效应

单色光和分子相互作用所产生的散射现象可以用光子(粒子)与分子的碰撞来解释，即拉曼光谱效应的量子理论描述。频率为 ν_0 的单色光的光子能量为 $h\nu_0$ ，其中 h 为普朗克常数，当光子 $h\nu_0$ 和分子作用时，可能发生弹性和非弹性两种碰撞。Fig. 1-1 为单色光光子和分子作用的散射光谱描述图。在弹性碰撞过程中，光子与分子之间不发生能量的交换，即光子仅改变运动方向而不改变频率，这种散射过程被称为瑞利散射。在非弹性碰撞过程中，光子与分子之间发生了能量的交换，光子的运动方向和频率皆发生了变化。处于 $E_v=0$ 基态的分子受入射光子 $h\nu_0$ 的激发而跃迁到一个受激虚态(实际上该受激虚态是不稳定的，因此是不存在的)，随后分子跃迁返回到基态 $E_v=0$ ，此过程对应于弹性碰撞，跃迁过程中放出的光子的能量仍为 $h\nu_0$ ，即瑞利散射线。而当处于虚态的分子跃迁到 $E_v=1$ ，则对应于

非弹性碰撞，光子中的部分能量传递给分子，散射光子能量等于 $h(\nu_0 - \nu)$ ，这通常称为拉曼散射斯托克斯线；相类似的过程也可能发生在处于 $E_v=1$ 的分子受入射光子 $h\nu_0$ 的激发而跃迁到受激虚态，然后又跃迁到基态 $E_v=0$ ，光子从分子得到部分能量而变为 $h(\nu_0 + \nu)$ ，称为反斯托克斯线。由此可见拉曼散射光子的频率都是相对于入射光子的频率而言，因此拉曼光谱中得到的振动谱峰的频率为拉曼位移(Raman shift)，并且拉曼光谱的斯托克斯线和反斯托克斯线对称分布在瑞利线的两侧[9-11]。

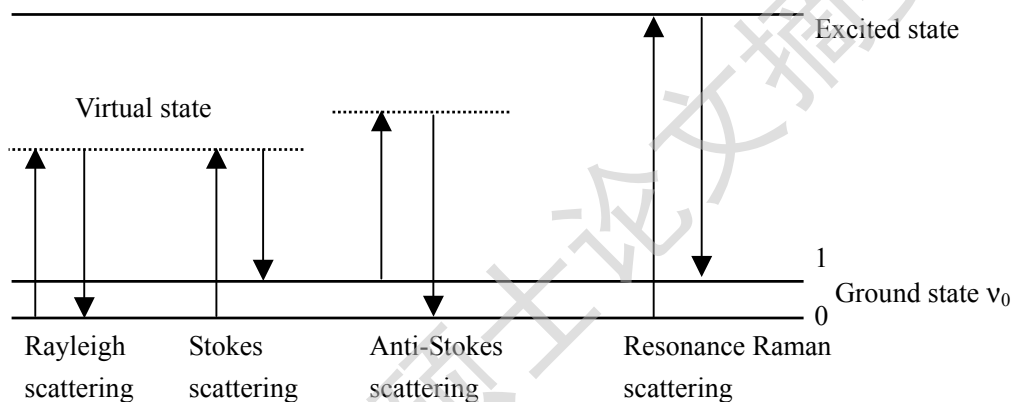


Fig. 1-1 Schematic diagram for Raman and Rayleigh scattering

根据经典理论的描述，可将单色光与分子相互作用所产生的散射现象用光波电场和分子的相互作用来解释，频率为 ν_0 的光的电场强度为 $E = E_0 \cos 2\pi\nu_0 t$ ，当它入射到分子表面时，分子可能被入射光电场极化而产生诱导偶极距 μ ，

$$\mu = \alpha_0 E_0 \cos 2\pi\nu_0 t + \frac{1}{2} (\partial\alpha / \partial Q)_0 Q_0 E_0 \{ \cos [2\pi(\nu_0 + \nu)t] + \cos [2\pi(\nu_0 - \nu)t] \} \quad (1-1-1)$$

可见分子的诱导偶极距以三种频率辐射，第一项表示以不变频率 ν_0 辐射，对应于瑞利散射或弹性散射；第二项代表拉曼或非弹性散射，以频率为 $\nu_0 - \nu$ 和 $\nu_0 + \nu$ 辐射拉曼光子，它们又分别对应于拉曼散射的斯托克斯和反斯托克斯线。式中 α 为分子的极化率， Q 为分子振动的简正坐标， $(\partial\alpha / \partial Q)_0$ 则是 α 随简正坐标 Q 改变而变化的速率，只有该项不等于零，吸附的分子才具有 Raman 活性。

斯托克斯和反斯托克斯线的强度可分别表示为：

$$I_{k,i,j}^{stokes} = \frac{2\pi^2 h}{c} \times \frac{(\nu_0 - \nu)^4}{\nu [1 - \exp(-h\nu/kT)]} g_\nu \left(\frac{\partial \alpha_{ij}}{\partial Q_k} \right)_0^2 \quad (1-1-2)$$

$$I_{k,i,j}^{anti-stokes} = \frac{2\pi^2 h}{c} \times \frac{(\nu_0 + \nu)^4}{\nu [\exp(-h\nu/kT)]} g_\nu \left(\frac{\partial \alpha_{ij}}{\partial Q_k} \right)_0^2 \quad (1-1-3)$$

其中， c 是光速， ν 是简正振动频率， T 是样品的热力学温度， g_ν 是给定分子的简并度， Q_k 是分子振动的简正坐标，两者之间的比值符合[12]：

$$\frac{I_{anti-stokes}}{I_{stokes}} = \frac{(\nu_0 + \nu)^4}{(\nu_0 - \nu)^4} \exp(-h\nu/kT) \quad (1-1-4)$$

升高温度有利于增强反斯托克斯线，样品温度固定，拉曼位移 $\nu_0 - \nu$ 越大， $I_{anti-stokes}/I_{stokes}$ 越小。

通过上述对拉曼散射过程的描述，可以发现拉曼散射涉及到一个二次光子过程，由于受激虚态是不稳定的，因此拉曼过程发生的几率十分小，其散射强度很弱。在没有表面增强或共振增强的情况下，一般分子的微分拉曼散射截面只有甚至低于 $10^{-29} \text{ cm}^2 \text{ sr}^{-1}$ ，所以对于单分子层的吸附物种来说，如果使用常规的拉曼谱仪，其拉曼信号强度一般低于 1 光子计数/秒(cps)，这使得大多数吸附物种的非增强的拉曼信号强度都低于常规谱仪的检测灵敏度，因此检测灵敏度低是制约拉曼光谱应用发展的主要因素。

§1.1.3 拉曼光谱的发展

拉曼光谱由于拉曼散射信号弱，对于拉曼谱仪的灵敏度和分辨率要求高，因此在实验技术上存在着许多困难，导致在随后的四十年内发展十分缓慢。从上个世纪六十年代起，人们从谱仪检测性能的改善和拉曼散射信号的增强入手，大大推动了拉曼光谱的发展。

在拉曼光谱实验研究阶段的早期，检测技术比较落后。例如，使用棱镜作为分光元件，而导致仪器大型化且分辨率较低；采用照相感光纸记录拉曼光谱；作为激发光源的汞弧灯的能量较低，导致采谱时间长达数小时甚至数十天，样品用量大且荧光干扰明显，只限于测试无色液体样品。二十世纪六十年代初，激光技术的问世给拉曼光谱带来了新的生机并很

Degree papers are in the "[Xiamen University Electronic Theses and Dissertations Database](#)". Full texts are available in the following ways:

1. If your library is a CALIS member libraries, please log on <http://etd.calis.edu.cn/> and submit requests online, or consult the interlibrary loan department in your library.
2. For users of non-CALIS member libraries, please mail to etd@xmu.edu.cn for delivery details.

厦门大学博硕士学位论文摘要库